

## Research Article

# Experimental Study on the Shear Strength of Dune Sand Concrete Beams

Zhiqiang Li , Rui Ma , and Gang Li 

College of Water and Architectural Engineering, Shihezi University, Shihezi 832003, China

Correspondence should be addressed to Zhiqiang Li; [zhiqiangli2023@163.com](mailto:zhiqiangli2023@163.com) and Gang Li; [gangli@shzu.edu.cn](mailto:gangli@shzu.edu.cn)

Received 2 July 2019; Revised 13 December 2019; Accepted 16 December 2019; Published 9 January 2020

Academic Editor: Giovanni Minafò

Copyright © 2020 Zhiqiang Li et al. This is an open access article distributed under the Creative Commons Attribution License, which permits unrestricted use, distribution, and reproduction in any medium, provided the original work is properly cited.

An experimental study was performed to investigate the shear strength of concrete beams made with dune sand (DS) from the Gurbantungut Desert in the Chinese province of Xinjiang. The test consisted of 3 series of beams which explored the shear properties of dune sand concrete (DSC) beams. The failure mode, crack pattern, load deflection, and stirrup strain were investigated. Meanwhile, the effect of shear span-to-depth ratio ( $a/d$ ), stirrup ratio, and dune sand replacement ratio on the shear strength of DSC beams was discussed. The results showed that the dune sand replacement ratio had insignificant influence on the failure mode of beams, so it was feasible to use DS to fabricate beams in regions of Xinjiang in China. Furthermore, the measured shear strengths of the DSC beams were compared with the calculated values of current design codes, and the results indicated that the shear strength of DSC beams was not precisely predicted by current design codes. Therefore, a modified formula was proposed to calculate the shear strength of DSC beams.

## 1. Introduction

The province of Xinjiang is located in the northwest of China, and nearly a quarter of Xinjiang is covered with DS due to dry continental climatic conditions [1]. The region of Xinjiang is characterized by a lack of natural fine aggregate resources. However, this region hosts a multitude of construction activities that require many aggregates for the one-belt-one-road policy. At the same time, transporting aggregates from other regions is expensive and uneconomical. Previous works of literature [2, 3] have shown that sand concrete can be applied in areas where aggregate resources are in short supply for economic or environmental reasons. Therefore, using DS as a fine aggregate resource will provide an alternative solution to these problems.

The content and fineness of aggregates have significant influence on the mechanical properties of concrete (strength, workability, and shrinkage). Therefore, numerous studies on the various properties of DSC were carried out. The early research on concrete made with DS from Algeria was carried out by Bédérina et al. [4], and their study mainly investigated the promotion of local DS and reuse of various wastes. The

results showed that better mechanical properties could be obtained by mixing dune and river sands in predetermined proportions. Guettala and Mezghiche [5, 6] repeated the study by adding dune sand powder (DSP) as a part mass addition to Portland cement, and the results proved that DSP presented a partial pozzolanic reactivity. Belferrag et al. [7] repeated the study by using waste metal fibers to improve the compressive strength of DSC and cement mortar.

Bederina et al. [8, 9] investigated the lightweight concrete made with DS by adding wood shavings to form a lightweight sand concrete and to strengthen its thermal properties, and the results showed that the DSC exhibited good thermal conductivities. Amel et al. [10] studied the mechanical and thermal lightweight concrete properties by adding DS and pumice. Damene et al. [11] investigated the porosity, compressive strength, and thermal conductivity of lightweight cellular concrete by adding lime and aluminium content on elaborated concrete made with southern Algeria dune sand.

Bouziani et al. [12] optimized the content of DS in construction in Saharan regions of Algeria, and this study was repeated by Hadjoudja et al. [13] and Zaitri et al. [14] by adding fiber and limestone rock in DSC.

Benmerioul et al. [15] studied the compressive strength, workability, and shrinkage of self-compacting concrete made utilizing ground DS. The aftereffects of this exploration demonstrated that the workability and shrinkage of concrete decreased with an increase in DS replacement levels; however, the short-term mechanical properties such as 28-day compressive strength improved.

The early research on concrete made with DS from China was carried by Zhang et al. [16], and their study was mainly about investigating the mechanical properties of mortar and concrete prepared from Tenggelu sand and Maowusu sand as fine aggregate. The test results showed that DS could be used as a fine aggregate in mortar and concrete for ordinary civil engineering, and the properties of DSC were different when the DS came from different desert regions. Jiang et al. [17] repeated the study to investigate the mechanical and durability properties and microstructure of mixtures made with DS, and the results suggested that the DS could be applied as substitution for ordinary concrete in hydraulic engineering.

Al-Harthy et al. [18] studied the mechanical properties and workability of concrete made with DS in Oman, and tests found that the mechanical strength of DSC is similar to that of conventional natural aggregate concrete (NAC), when the concrete mixes were designed properly.

Luo et al. [19] studied the properties of concrete made with DS from Australian deserts, and results showed that the performance of DSC would vary according to the S/C ratio.

Abu Seif [20] presented the engineering properties of concrete made with DS from Egypt. The results of the tests indicated the compressive strength of concrete decreased with increasing DS content.

Alhozaimy et al. [21, 22] investigated compressive strength and microstructure properties of concrete and mortar containing white sand and DS from Saudi Arabia, and results indicated that the compressive strength of mortar increased as the level of replacement increased under autoclave curing. Alawad et al. [23] repeated the study to analyze the microstructure of DSC by SEM, EDX, XRD, DAT, and TGA. Abu Seif et al. [24] studied the mortar and concrete made with DS in the area of Saudi Arabia, and tests showed that the compressive strength and workability of the DSC and cement mortar were both suitable when the volume of sand does not exceed 50% of the total fine aggregate.

Lee et al. [25] investigated the drying shrinkage cracking of DSC and revealed the correlation between compressive strength and DS/FA. Park et al. [26] evaluated the rheological properties of concrete made with DS and analyzed the plastic viscosity of concrete.

Wang et al. [27] investigated the properties of concrete-filled steel tubular (CFST) stub columns and beams using DS as part of the fine aggregate. Ren et al. [28] studied the performance of CFST stub columns under axial compression, and tests indicated that it was possible to use DS instead of conventional sand to fabricate CFST columns in the desert areas of China.

Beam is one of the important components of the structure, so numerous studies have been carried out in previously literatures [29–35]. However, comparably rare

research on the shear behaviour of DSC beams has been carried out. Therefore, the primary objective of this study was to investigate  $a/d$ , stirrup ratio, and dune sand replacement ratio on the shear strength of DSC beams. This study also investigated the failure mode, crack pattern, load deflection, and stirrup strain of DSC beams. Furthermore, a modified formula was proposed to calculate the shear strength of DSC beams.

## 2. Materials and Experimental Methods

**2.1. Materials and Mixture Proportions.** In this study, all the specimens were cast with a target cube compressive strength of 40 MPa. Ordinary Portland cement with grade 42.5 and the fly ash with grade I were used for all the concrete mixtures according to the Chinese Code GB50010-2010 [36]. The fine and coarse aggregates used were river natural sand taken from the Manas River in Xinjiang province of China. The fine aggregate's size ranged from 0.4 mm to 2.5 mm, and coarse aggregate's size ranged from 5 mm to 20 mm. The DS used in the concrete mixtures was taken from the Gurbantunggut Desert in Xinjiang province. The properties of DS are presented in Table 1. The HSC brand superplasticizer was used in all the mixtures. The properties of HSC is presented in Table 2. The water used was tap water. The mix proportion of DSC is presented in Table 3.

A standard rotating drum mixer was used to mix all the materials. And the specimens were fabricated according to mix proportion in Table 3. Both the concrete cubes and beams were placed in appropriate molds. When the concrete was vibrated, the specimens were cured in a natural environment until 28 days. The compressive strengths ( $f_{cu}$ ), tensile strength ( $f_t$ ), and elastic modulus ( $E_c$ ) were determined according to Xiao et al. [37], Chinese Code GB50010-2010 [36], and ACI318 [38], as shown in Table 4.

**2.2. Details of Test Beams.** 3 series of beams (see Table 4 and Figure 1) were designed and constructed using DSC. For series B1, the dune sand replacement ratio and the stirrup ratio were the same, while  $a/d$  ranged from 1.0 to 3.0. For series B2,  $a/d$  and the stirrup ratio were the same, while the dune sand replacement ratio ranged from 0% to 80%. For series B3,  $a/d$  and the dune sand replacement ratio were the same, while the stirrup ratio ranged from 0.45% to 0.67%.

$a/d$ , dune sand replacement ratio, stirrup ratio, and reinforcement ratio all conform to Chinese Code GB50010-2010 [36].  $a/d$  is the ratio of shear span to depth; the "dune sand replacement ratio" is the ratio of dune sand to fine aggregate; the "stirrup ratio" is  $r_{sv} = (A_{sv}/bs)$ , where  $A_{sv}$  is the area of the stirrup,  $b$  is the width of beam, and  $s$  is the stirrup spacing; the "reinforcement ratio" is  $\rho_w = (A_s/A_c)$ , where  $A_s$  is the area of all longitudinal reinforcement and  $A_c$  is the cross-sectional area of a beam.

All the beams were of cross section 150 mm × 300 mm, and all the beams were defined by the reinforcement ratio  $\rho_w = 0.96\%$  ( $2\phi 16$ ). The beams tested in series B1 had a clear length of 1300 mm, 1700 mm, 2100 mm, and 2500 mm due to different  $a/d$ , while the beams tested in series B2 and series B3 had the same clear length of 1300 mm. The

TABLE 1: The chemical composition of dune sand (Gurbantunggut Desert).

SiO <sub>2</sub>	Al <sub>2</sub> O <sub>3</sub>	Fe <sub>2</sub> O <sub>3</sub>	Na <sub>2</sub> O	CaO	K <sub>2</sub> O	MgO	FeO	TiO <sub>2</sub>	P <sub>2</sub> O <sub>5</sub>	MnO
67.1%	17.9%	1.35%	4.94%	4.22%	3.48%	0.84%	0.06%	0.02%	0.05%	0.04%

TABLE 2: Superplasticizer properties (HSC).

HSC	Shape	Colour	pH	Density
Properties	Liquid	Transparent	6–8	1.08 ± 0.02

TABLE 3: The mix proportion of DSC.

Specimens	Water-cement ratio	Sand ratio	Material consumption (kg/m <sup>3</sup> )						
			Water	Cement	Fly ash	HSC	Coarse aggregate	Fine aggregate	DS
DSC-0	0.40	0.30	160	370	30	1.6	1288	552	0
DSC-20	0.40	0.30	160	370	30	1.6	1288	441.6	110.4
DSC-40	0.40	0.30	160	370	30	1.6	1288	331.2	220.8
DSC-60	0.40	0.30	160	370	30	1.6	1288	220.8	331.2
DSC-80	0.40	0.30	160	370	30	1.6	1288	110.4	441.6

properties of longitudinal reinforcement and stirrup are shown in Table 5.

**2.3. Test Setup and Measurements.** The test setup is shown in Figure 1(a), and the details of test beam are shown in Figure 1(b). The beams were tested in four-point bending. The supports were placed to allow for deflection, 150 mm from each end of the beam. The load was transferred to the load points via a steel I-beam. The load was applied with a rate of 0.50 mm/min. All the beams were loaded until failure.

The linear variance displacement transducer (LVDT) used to measure the displacement was placed under the center of the beam, and the strain gauges were connected to the stirrup to measure strain (see Figure 1). Data were recorded by a data acquisition machine, and the cracks formed on the surface of the beam were marked by manual record.

### 3. Results

**3.1. Failure Mode and Crack Pattern.** The experimentally obtained crack patterns of series B1 are plotted in Figure 2. The figure showed that  $a/d$  had significant influence on the failure mode of beams. The beam B1-1 failed in diagonal shear; B1-2, B1-3, and B1-4 failed in bending-shear; and B1-5 failed in bending.

The main failure process of beam B1-1 could be described as follows: when the load was about 30% of ultimate strength, short diagonal cracks propagated at the bottom of the beam between the load points and support. With the load increase, the diagonal crack extended towards the load points. Finally, when the load was close to the ultimate strength, one crack led to sudden and catastrophic failure, and the failure was solely due to the diagonal tension crack that propagated between the load point and the support.

The main failure process of beams B1-2, B1-3, and B1-4 could be described as follows: when the load was about 30% of ultimate strength, short vertical cracks propagated at the bottom of the beam between the load points. With the load increase, the diagonal cracks appeared between the load points and support. Finally, when the load was close to the ultimate strength, the concrete in the zone of the beam near the load plates was crushed, and the failure was due to diagonal tension cracks and bending cracks.

For the beam of B1-5, the main failure process was similar to that of B1-2, B1-3, and B1-4, but the bending cracks were evident, and the failure was due to bending cracks.

In a word, more and more vertical cracks formed with the increase of  $a/d$  in the test beams, and the ultimate strength was reduced with the increase of  $a/d$ .

The experimentally obtained crack patterns of series B2 are plotted in Figure 3. The figure showed that all of the beams failed in bending-shear, and the main failure process and crack patterns of series B2 were similar to that of B1-2. The dune sand replacement ratio had insignificant influence on the failure mode of beams because the DSC strength of series B2 was close and the bearing capability of the beams was approximately equal.

The experimentally obtained crack patterns of series B3 are plotted in Figure 4. The figure showed that the stirrup ratio had insignificant influence on the failure mode of beams. All of the beams failed in bending-shear, and the main failure process of series B3 was similar to that of B1-2. However, the crack patterns of series B3 were different with B1-2. More and more diagonal cracks formed with the increase of stirrup ratio, and the ultimate strength was increased with the increase of stirrup ratio.

**3.2. Load-Deflection Curve.** The load-deflection curves of beams are grouped to examine  $a/d$ , dune sand replacement ratio, and stirrup ratio as shown in Figure 5.

TABLE 4: Details of the experimental beams.

Series	Specimens ID	Clear length $l_n$ (mm)	Concrete compression strength $f_{cu}$ (MPa)	Concrete splitting strength $f_t$ (MPa)	$E_c$ ( $10^4$ N/mm <sup>2</sup> )	$a/d$	Dune sand replacement ratio $r$ (%)	Stirrup ratio $r_{sv}$
B1	B1-1	1300	42.50	2.53	3.12	1.0	80	$r_{sv} = 0.45\%$
	B1-2	1300	42.73	2.54	3.12	1.5	80	$r_{sv} = 0.45\%$
	B1-3	1700	37.59	2.38	3.12	2.0	80	$r_{sv} = 0.45\%$
	B1-4	2100	37.59	2.38	3.12	2.5	80	$r_{sv} = 0.45\%$
	B1-5	2500	37.59	2.38	3.12	3.0	80	$r_{sv} = 0.45\%$
B2	B2-1	1300	45.25	2.77	3.47	1.5	0	$r_{sv} = 0.45\%$
	B2-2	1300	42.19	2.64	3.47	1.5	20	$r_{sv} = 0.45\%$
	B2-3	1300	41.5	2.58	3.63	1.5	40	$r_{sv} = 0.45\%$
	B2-4	1300	39.1	2.46	3.18	1.5	60	$r_{sv} = 0.45\%$
	B2-5	1300	42.73	2.54	3.12	1.5	80	$r_{sv} = 0.45\%$
B3	B3-1	1300	42.73	2.54	3.12	1.5	80	$r_{sv} = 0.45\%$ ( $\phi 8@150$ )
	B3-2	1300	37.59	2.38	3.12	1.5	80	$r_{sv} = 0.56\%$ ( $\phi 8@120$ )
	B3-3	1300	37.59	2.38	3.12	1.5	80	$r_{sv} = 0.67\%$ ( $\phi 8@100$ )

\*The specimens designated B1-2, B2-5, and B3-1 were actually the same specimen belonging to different series.

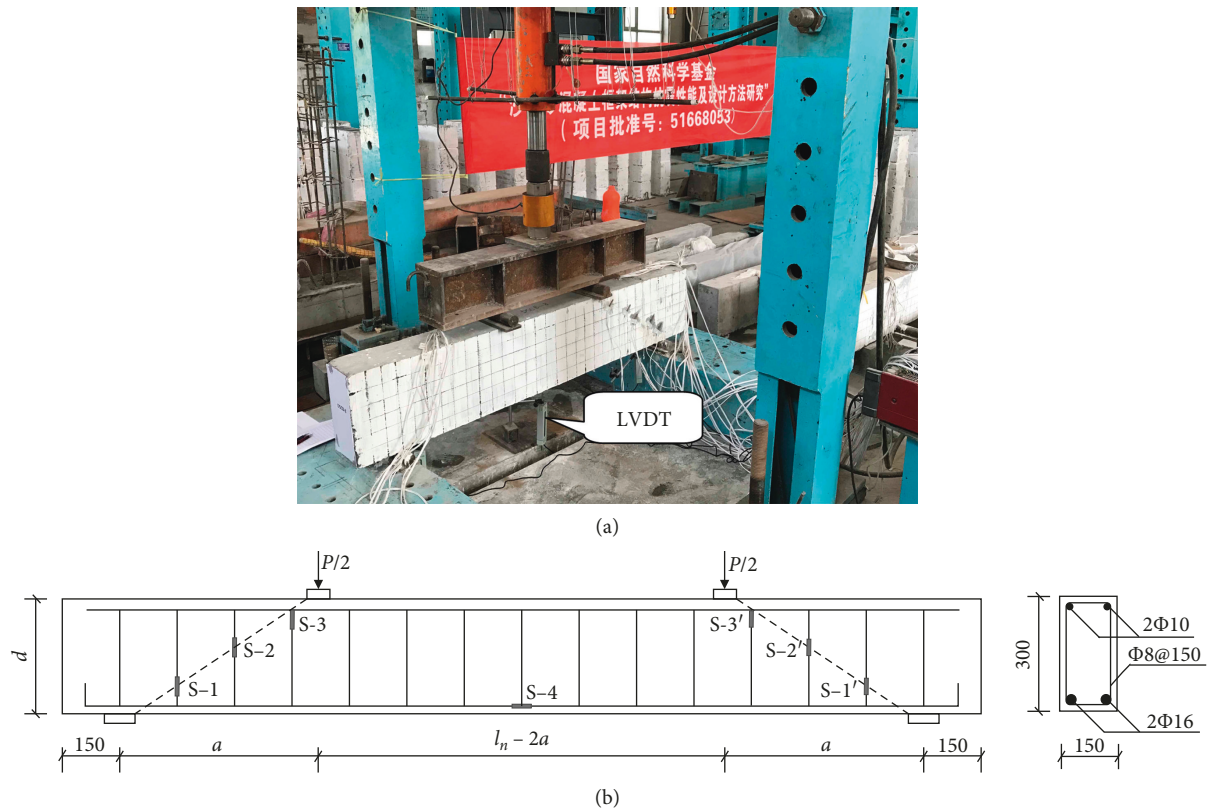


FIGURE 1: Test setup and details of test beams. (a) Test setup and load pattern. (b) Cross sections, reinforcement layout, and location of strain gauges on the test beams.

Figure 5(a) shows the load-deflection curves of series B1. When  $a/d$  increased from 1.0 to 3.0, the ultimate strength of DSC beams significantly decreased; however, the damaged deflection significantly increased.

Figure 5(b) shows the load-deflection curves of series B2. When the dune sand replacement ratio increased from 0% to 80%, the ultimate strength of DSC beams insignificantly decreased and the damaged deflection insignificantly increased.

TABLE 5: Properties of longitudinal reinforcement and stirrup.

Diameter (mm)	Yield strength $f_y$ (MPa)	Ultimate strength $f_u$ (MPa)	Elastic modulus of steel $E_s$ (MPa)
8	441	615	$200 \times 10^3$
16	430	611	$200 \times 10^3$

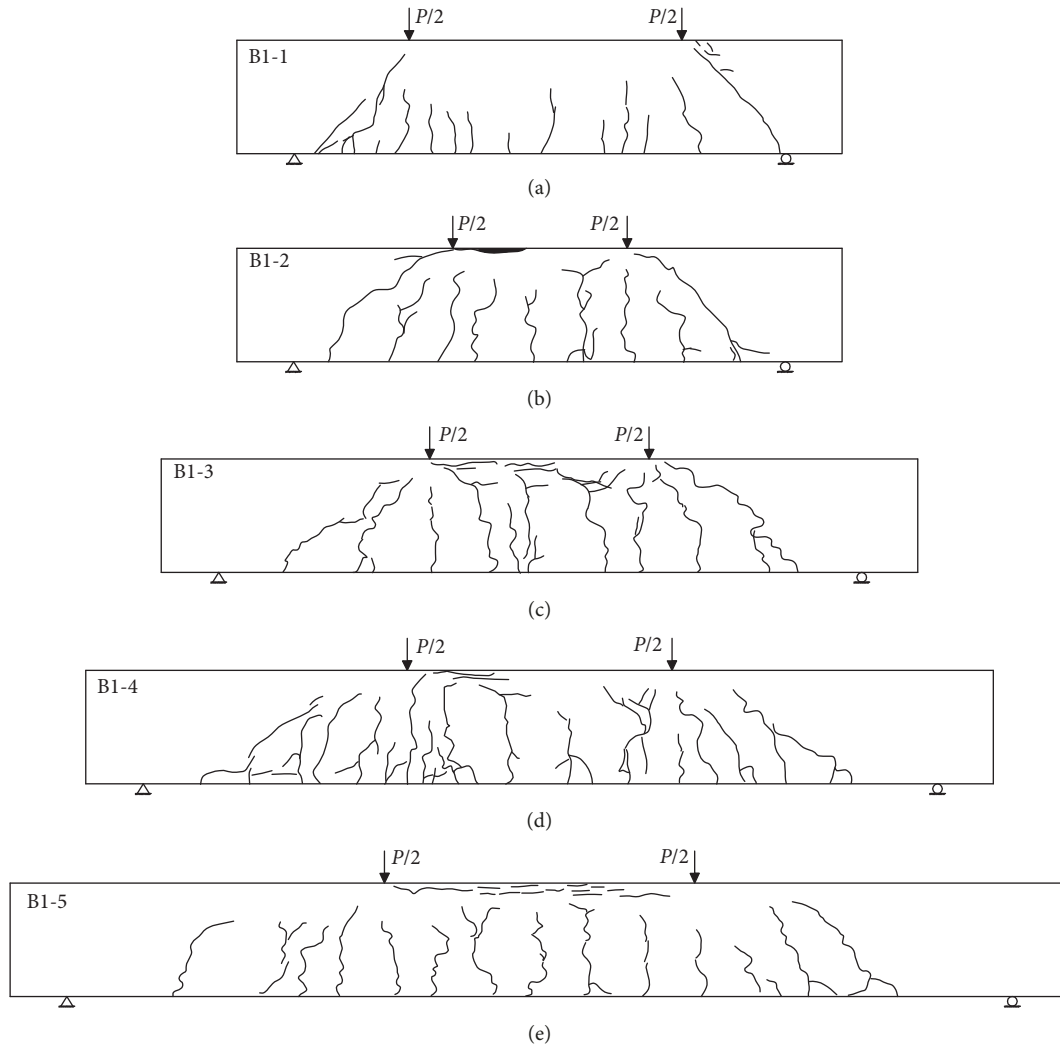


FIGURE 2: Crack patterns of series B1: (a) B1-1; (b) B1-2; (c) B1-3; (d) B1-4; (e) B1-5.

In a word, the dune sand replacement ratio could not improve the ultimate strength and damaged deflection of series B2.

Figure 5(c) shows the load-deflection curves of series B3. When the stirrup ratio increased from 0.45% to 0.56%, the ultimate strength of DSC beams significantly increased and the damaged deflection insignificantly decreased. However, when the stirrup ratio increased from 0.56% to 0.67%, the ultimate strength and damaged deflection of B3-3 were almost the same with those of B3-2.

**3.3. Stirrup Strain.** The development of stirrup strain of S-3 for specimens is presented in Figure 6.

Figure 6(a) shows the load stirrup strain curves of series B1. There is significant difference in stirrup strain values

among series B1.  $a/d$  significantly decreased the stirrup strain and ultimate strength of the beams when  $a/d$  increased from 1.0 to 3.0.

Figure 6(b) shows the load stirrup strain curves of series B2. There is no significant difference in stirrup strain values among series B2, except for B2-5. The dune sand replacement ratio insignificantly decreased the stirrup strain and ultimate strength of the beams when the dune sand replacement ratio increased from 0% to 60%. However, when the dune sand replacement ratio increased from 60% to 80%, the stirrup strain of B2-5 was significantly smaller than the other beams.

Figure 6(c) shows the load stirrup strain curves of series B3. There is significant difference in stirrup strain values among series B3. The stirrup ratio significantly increased the

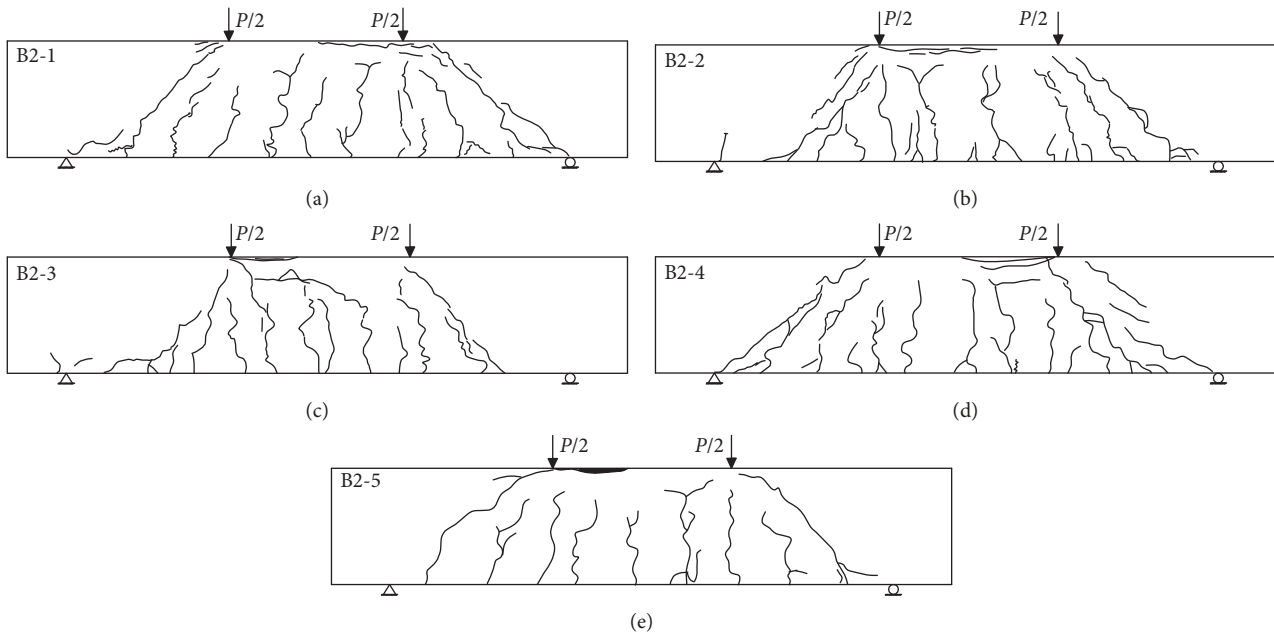


FIGURE 3: Crack patterns of series B2: (a) B2-1; (b) B2-2; (c) B2-3; (d) B2-4; (e) B2-5.

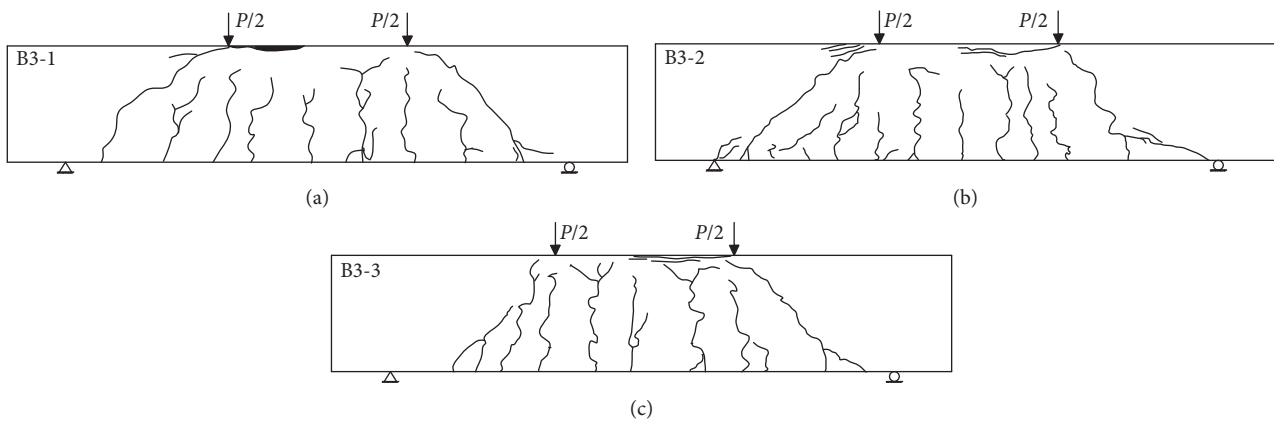


FIGURE 4: Crack patterns of series B3: (a) B3-1; (b) B3-2; (c) B3-3.

stirrup strain and ultimate strength of the beams when the stirrup ratio increased from 0.45% to 0.67%.

## 4. Discussion

**4.1. Effect of  $a/d$  on Shear Strength.** For Series B1, when the stirrup ratio and dune sand replacement ratio were the same, the shear strengths of the beams decreased with the increase of  $a/d$ , as shown in Figure 7. When the  $a/d$  was 1.5, 2.0, 2.5, and 3.0, compared with B1-1 ( $a/d = 10$ ), the shear strengths of the test beams decreased by 7.46%, 21.97%, 37.64%, and 41.10%, respectively. The phenomenon that the shear strengths of the beams decreased with the increase of  $a/d$  was similar to the previous studies [39, 40].

**4.2. Effect of Dune Sand Replacement Ratio on Shear Strength.** For series B2, when the stirrup ratio and  $a/d$  were the same, the shear strengths of the beams decreased with the increase

of the dune sand replacement ratio, as shown in Figure 8. When the dune sand replacement ratio was 20%, 40%, 60%, and 80%, compared with B2-1 ( $r=0\%$ ), the shear strengths of the test beams decreased by 4.79%, 6.19%, 6.72%, 6.80%, respectively. It indicated that the dune sand replacement ratio had insignificant influence on the shear strengths of the beams, and the results were consistent with the failure mode of beams of series B2. Therefore, it was feasible to use dune sand to replace normal sand to fabricate beams in regions of Xinjiang in China.

**4.3. Effect of Stirrup Ratio on Shear Strength.** For Series B3, when  $a/d$  and dune sand replacement ratio were the same, the shear strengths of the beams increased with increasing stirrup ratio, as shown in Figure 9. When the stirrup ratio was 0.56% and 0.67%, compared with B3-1 ( $r_{sv}=0.45\%$ ), the shear strengths of the test beams increased by 12.02% and 18.51%, respectively. It indicated that the shear strengths of

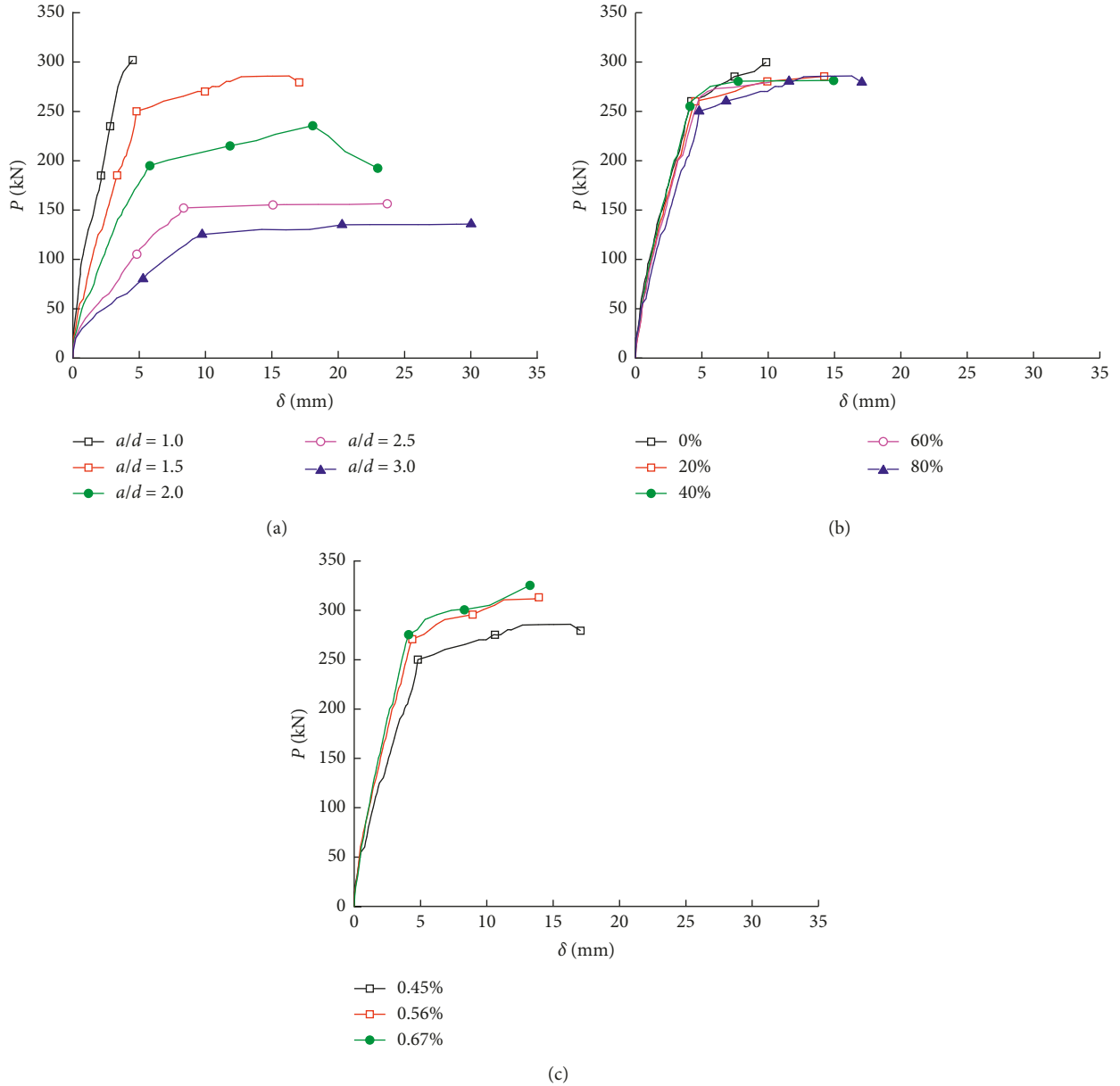


FIGURE 5: Load-deflection curves of beams: (a) series B1; (b) series B2; (c) series B3.

the beams increased with increasing stirrup ratio, and the phenomenon was similar to the previous studies [41, 42].

**4.4. Comparison between the Measured Values and the Calculated Values by Current Design Codes.** To date, no mathematical formula could be used as standard method to calculate the shear strength of DSC beams, so the formula in GB50010-2010 [36] was adopted, as shown in the following equation:

$$V_{GB} = V_c + V_{sv} = \frac{1.75}{1 + \lambda} f_t b h_0 + f_{yv} \frac{A_{sv}}{s} h_0, \quad (1)$$

where  $V_{GB}$  is the shear strength of the beam;  $V_c$  is the shear force provided by the concrete;  $V_{sv}$  is the shear force

provided by the stirrup;  $\lambda$  is the shear span-to-depth ratio;  $f_t$  is the tensile strength of DSC;  $b$  and  $h_0$  are the width and the effective depth of beam;  $f_{yv}$  and  $A_{sv}$  are the yield strength and cross section area of stirrup; and  $s$  is the stirrup spacing in the shear span.

The shear strengths of beams calculated by GB50010-2010 [36] and ACI318 [38] are shown in Table 6. It can be seen that the average ratio of  $V_{GB}/V_{u,exp}$  is 1.167, and the average ratio of  $V_{ACI}/V_{u,exp}$  is 1.07.  $V_{u,exp}$  is the shear strength of test;  $V_{ACI}$  is the shear strength calculated by ACI318 [38]. The results indicate that the shear strengths calculated by current design codes [36, 38] are not safe. Therefore, equation (1) needs to be modified.

The DSC was the main factor for changing the shear strength of concrete beam. Hence, the corresponding

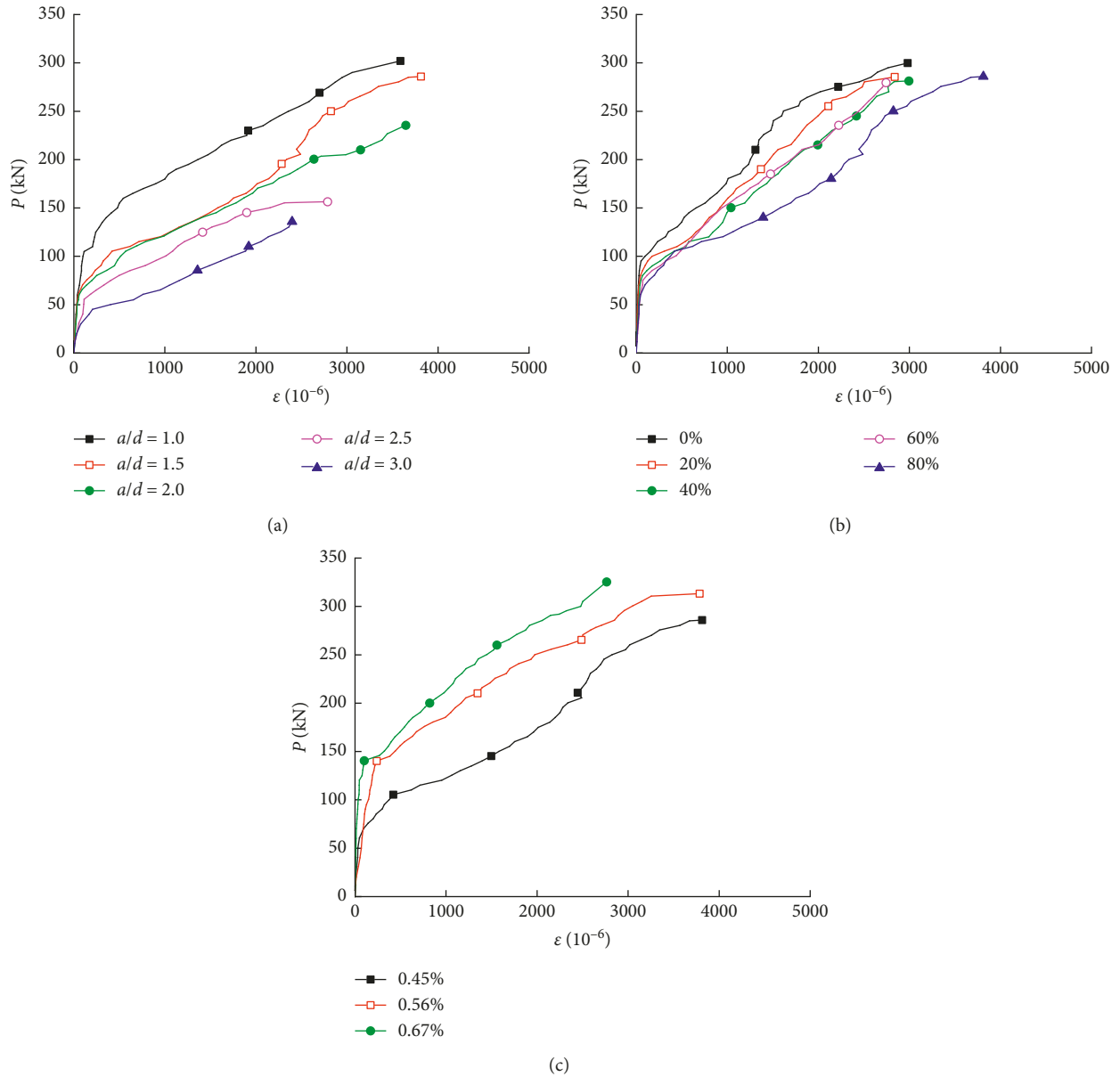


FIGURE 6: Load stirrup strain curves of beams: (a) series B1; (b) series B2; (c) series B3.

correction of  $V_c$  could be made in equation (1) to make it more suitable for the shear calculation of desert sand concrete beam [43], as shown in the following equation:

$$V_{GB}^1 = \frac{a + br + cr^2 + dr^3}{e + f\lambda + g\lambda^2} f_t b h_0 + \frac{f_{yv} A_{sv} h_0}{s}, \quad (2)$$

where  $V_{GB}^1$  is the modified shear strength of the beam;  $a, b, c, d, e, f,$  and  $g$  are resistance coefficients of concrete, and they can be obtained by applying Origin2019 software for regression analysis; and  $r$  is the dune sand replacement ratio.

When  $a = 1.502, b = -0.889, c = 2.337, d = 1.733, e = 3.737, f = -3.744,$  and  $g = 2.133,$  the average ratio of  $V_{GB}^1/V_{u,exp}$  is 0.971, and the average ratio of  $V_{GB}^1/V_{ACI}$  is 0.922, as shown in Table 6. The results indicate that the

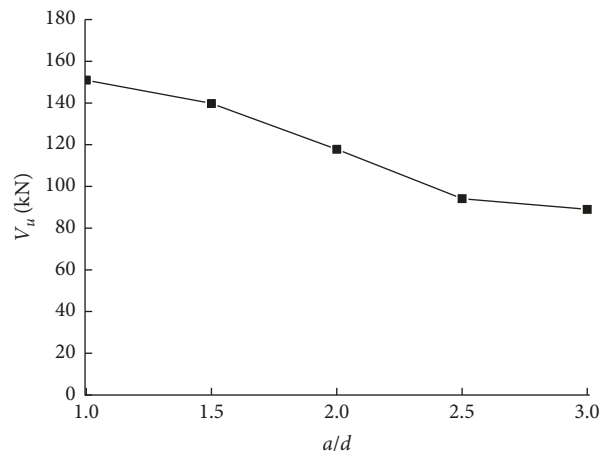


FIGURE 7: Relationship of shear strength and  $a/d$ .

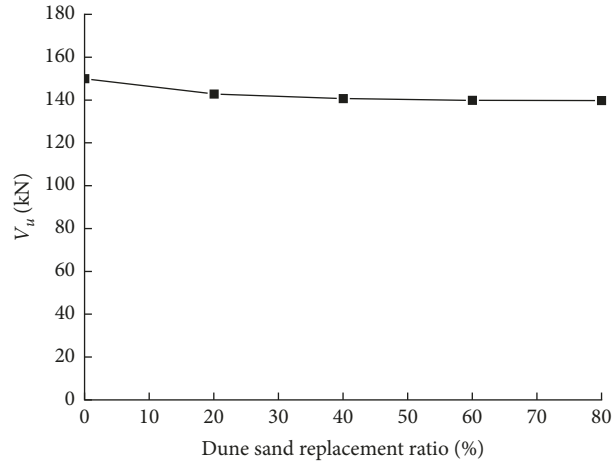


FIGURE 8: Relationship of shear strength and dune sand replacement ratio.

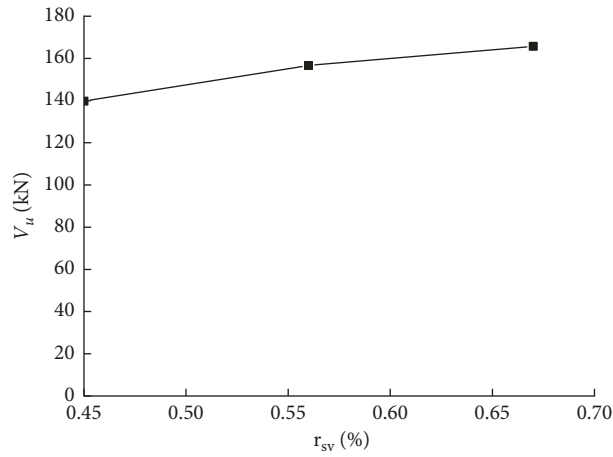


FIGURE 9: Relation of shear strength and  $r_{sv}$ .

TABLE 6: Comparison of test results with the calculated values by current design codes.

Specimens	$V_{u,exp}$ (kN)	$V_{GB}$ (kN)	$V_{ACI}$ (kN)	$V_{GB}/V_{u,exp}$	$V_{ACI}/V_{u,exp}$	$V_{GB}^1$ (kN)	$V_{GB}^1/V_{u,exp}$	$V_{GB}^1/V_{ACI}$
B1-1	151.00	173.10	140.46	1.15	0.93	150.06	0.99	1.07
B1-2	139.73	160.68	138.61	1.15	0.99	135.26	0.97	0.98
B1-3	117.82	138.44	134.50	1.18	1.14	109.38	0.93	0.81
B1-4	94.15	130.11	133.73	1.38	1.42	98.27	1.04	0.73
B1-5	88.94	123.86	133.18	1.39	1.50	92.08	1.04	0.69
B2-1	149.92	161.56	139.89	1.08	0.93	139.97	0.93	1.00
B2-2	142.74	157.74	138.33	1.11	0.97	133.43	0.94	0.96
B2-3	140.64	155.98	137.97	1.11	0.98	132.43	0.94	0.96
B2-4	139.84	152.45	136.69	1.09	0.98	130.92	0.94	0.96
B2-5	139.73	160.68	138.61	1.15	0.99	135.27	0.97	0.98
B3-1	139.73	160.68	138.61	1.15	0.99	135.27	0.97	0.98
B3-2	156.66	170.13	158.14	1.09	1.01	148.05	0.95	0.94
B3-3	165.73	190.16	180.41	1.15	1.09	168.08	1.01	0.93
AVG				1.167	1.07		0.971	0.922
C.o.V				0.101	0.183		0.039	0.110

shear strengths calculated by modified formula is safer, and the modified formula is consistent with the experimental results and ACI318 [38]. Consequently, the shear strength of DSC beams can be predicted by the modified formula in this paper. And the modified formula is

$$V_{GB}^1 = \frac{1.502 - 0.889r + 2.337r^2 + 1.733r^3}{3.737 - 3.744\lambda + 2.133\lambda^2} f_t b h_0 + \frac{f_{yv} A_{sv} h_0}{s} \quad (3)$$

## 5. Conclusions

Based on the results of a survey conducted by the authors, the following conclusions were drawn:

- (1) The failure process and crack pattern of DSC beam was similar to that of ordinary concrete beam. When  $a/d \leq 1$ , the beam failed in diagonal shear; when  $1.5 \leq a/d < 3.0$ , the beam failed in bending-shear; and when  $3.0 \leq a/d$ , the beam failed in bending.
- (2) With the increase of  $a/d$ , the ultimate strength and stirrup strain of DSC beams significantly decreased, and the damaged deflection significantly increased.
- (3) With the increase of dune sand replacement ratio, the ultimate strength and stirrup strain of DSC beams insignificantly decreased, and the damaged deflection insignificantly increased. However, the stirrup strain of B2-5 was significantly smaller than the other beams.
- (4) With the increase of stirrup ratio, the ultimate strength and stirrup strain of DSC beams significantly increased, and the damaged deflection insignificantly decreased. However, ultimate strength and damaged deflection of B3-3 were almost the same with those of B3-2.
- (5) The modified formula could be used to calculate the shear strength of DSC beams.
- (6) It was feasible to use DS to replace normal sand to fabricate beams in regions of Xinjiang in China.

## Data Availability

The data used to support the findings of this study are available from the corresponding author upon request.

## Conflicts of Interest

The authors declare that there are no conflicts of interest regarding the publication of this paper.

## Acknowledgments

This work was supported by the National Natural Science Foundation of China (grant no. 51668053).

## References

- [1] Y. Wang, D. Xiao, and Y. Li, "Temporal-spatial change in soil degradation and its relationship with landscape types in a desert-oasis ecotone: a case study in the Fubei region of Xinjiang Province, China," *Environmental Geology*, vol. 51, no. 6, pp. 1019–1028, 2007.
- [2] T. Bouziani, A. Benmounah, and M. Bédérina, "Statistical modelling for effect of mix-parameters on properties of high-flowing sand-concrete," *Journal of Central South University*, vol. 19, no. 10, pp. 2966–2975, 2012.
- [3] Z. Boudaoud and D. Breysse, "Étude des effets du cobroyage d'un sable et d'un clinker sur les propriétés d'un béton de sable," *Materials and Structures*, vol. 35, no. 5, pp. 310–316, 2002.
- [4] M. Bédérina, M. M. Khenfer, R. M. Dheilily, and M. Quéneudec, "Reuse of local sand: effect of limestone filler proportion on the rheological and mechanical properties of different sand concretes," *Cement and Concrete Research*, vol. 35, no. 6, pp. 1172–1179, 2005.
- [5] S. Guettala and B. Mezghiche, "Compressive strength and hydration with age of cement pastes containing dune sand powder," *Construction and Building Materials*, vol. 25, no. 3, pp. 1263–1269, 2011.
- [6] S. Guettala and B. Mezghiche, "Influence de l'addition du sable de dune en poudre au ciment sur les propriétés des bétons," *European Journal of Environmental and Civil Engineering*, vol. 15, no. 10, pp. 1483–1507, 2011.
- [7] A. Belferrag, A. Kriker, and M. E. Khenfer, "Improvement of the compressive strength of mortar in the arid climates by valorization of dune sand and pneumatic waste metal fibers," *Construction and Building Materials*, vol. 40, pp. 847–853, 2013.
- [8] M. Bederina, L. Marmoret, K. Mezreb, M. M. Khenfer, A. Bali, and M. Quéneudec, "Effect of the addition of wood shavings on thermal conductivity of sand concretes: experimental study and modelling," *Construction and Building Materials*, vol. 21, no. 3, pp. 662–668, 2007.
- [9] M. Bederina, B. Laidoudi, A. Goullieux, M. M. Khenfer, A. Bali, and M. Quéneudec, "Effect of the treatment of wood shavings on the physico-mechanical characteristics of wood sand concretes," *Construction and Building Materials*, vol. 23, no. 3, pp. 1311–1315, 2009.
- [10] C. L. Amel, E. H. Kadri, Y. Sebaibi, and H. Soualhi, "Dune sand and pumice impact on mechanical and thermal lightweight concrete properties," *Construction and Building Materials*, vol. 133, pp. 209–218, 2017.
- [11] Z. Damene, M. S. Goual, J. Houessou, R. M. Dheilily, A. Goullieux, and M. Quéneudec, "The use of southern Algeria dune sand in cellular lightweight concrete manufacturing: effect of lime and aluminium content on porosity, compressive strength and thermal conductivity of elaborated materials," *European Journal of Environmental and Civil Engineering*, vol. 22, no. 10, pp. 1273–1289, 2018.
- [12] T. Bouziani, M. Bederina, and M. Hadjoudja, "Effect of dune sand on the properties of flowing sand-concrete (FSC)," *International Journal of Concrete Structures and Materials*, vol. 6, no. 1, pp. 59–64, 2012.
- [13] M. Hadjoudja, M. M. Khenfer, H. A. Mesbah, and A. Yahia, "Statistical models to optimize fiber-reinforced dune sand concrete," *Arabian Journal for Science and Engineering*, vol. 39, no. 4, pp. 2721–2731, 2014.
- [14] R. Zaitri, M. Bederina, T. Bouziani, Z. Makhloufi, and M. Hadjoudja, "Development of high performances concrete

- based on the addition of grinded dune sand and limestone rock using the mixture design modelling approach,” *Construction and Building Materials*, vol. 60, pp. 8–16, 2014.
- [15] F. Benmerioul, A. Tafraoui, A. Makani, and S. Zaouai, “A study on mechanical properties of self-compacting concrete made utilizing ground dune sand,” *Revista Romana de Materiale—Romanian Journal of Materials*, vol. 47, no. 3, pp. 328–335, 2017.
- [16] G. Zhang, J. Song, J. Yang, and X. Liu, “Performance of mortar and concrete made with a fine aggregate of desert sand,” *Building and Environment*, vol. 41, no. 11, pp. 1478–1481, 2006.
- [17] C. H. Jiang, X. B. Zhou, G. L. Tao, and D. Chen, “Experimental study on the performance and microstructure of cementitious materials made with dune sand,” *Advances in Materials Science And Engineering*, vol. 2016, Article ID 2158706, 8 pages, 2016.
- [18] A. S. Al-Harthy, M. A. Halim, R. Taha, and K. S. Al-Jabri, “The properties of concrete made with fine dune sand,” *Construction and Building Materials*, vol. 21, no. 8, pp. 1803–1808, 2007.
- [19] F. J. Luo, L. He, Z. Pan, W. H. Duan, X. L. Zhao, and F. Collins, “Effect of very fine particles on workability and strength of concrete made with dune sand,” *Construction and Building Materials*, vol. 47, pp. 131–137, 2013.
- [20] E.-S. S. Abu Seif, “Assessing the engineering properties of concrete made with fine dune sands: an experimental study,” *Arabian Journal of Geosciences*, vol. 6, no. 3, pp. 857–863, 2013.
- [21] A. Alhozaimy, M. S. Jaafar, A. Al-Negheimish et al., “Properties of high strength concrete using white and dune sands under normal and autoclaved curing,” *Construction and Building Materials*, vol. 27, no. 1, pp. 218–222, 2012.
- [22] A. Alhozaimy, O. A. Alawad, M. S. Jaafar, A. Al-Negheimish, and J. Noorzai, “Use of fine ground dune sand as a supplementary cementing material,” *Journal of Civil Engineering and Management*, vol. 20, no. 1, pp. 32–37, 2014.
- [23] O. A. Alawad, A. Alhozaimy, M. S. Jaafar, F. N. A. Aziz, and A. Al-Negheimish, “Effect of autoclave curing on the microstructure of blended cement mixture incorporating ground dune sand and ground granulated blast furnace slag,” *International Journal of Concrete Structures and Materials*, vol. 9, no. 3, pp. 381–390, 2015.
- [24] E.-S. S. Abu Seif, A. R. Sonbul, B. A. H. Hakami, and E. K. El-Sawy, “Experimental study on the utilization of dune sands as a construction material in the area between Jeddah and Mecca, Western Saudi Arabia,” *Bulletin of Engineering Geology and the Environment*, vol. 75, no. 3, pp. 1007–1022, 2016.
- [25] E. Lee, S. Park, and Y. Kim, “Drying shrinkage cracking of concrete using dune sand and crushed sand,” *Construction and Building Materials*, vol. 126, pp. 517–526, 2016.
- [26] S. Park, E. Lee, J. Ko, J. Yoo, and Y. Kim, “Rheological properties of concrete using dune sand,” *Construction and Building Materials*, vol. 172, pp. 685–695, 2018.
- [27] W.-H. Wang, L.-H. Han, W. Li, and Y.-H. Jia, “Behavior of concrete-filled steel tubular stub columns and beams using dune sand as part of fine aggregate,” *Construction and Building Materials*, vol. 51, pp. 352–363, 2014.
- [28] Q.-X. Ren, K. Zhou, C. Hou, Z. Tao, and L.-H. Han, “Dune sand concrete-filled steel tubular (CFST) stub columns under axial compression: experiments,” *Thin-Walled Structures*, vol. 124, pp. 291–302, 2018.
- [29] G. Campione, A. Monaco, and G. Minafò, “Shear strength of high-strength concrete beams: modeling and design recommendations,” *Engineering Structures*, vol. 69, pp. 116–122, 2014.
- [30] L. Ombres and S. Verre, *Shear Performance of FRCM Strengthened RC Beams*, ACI Special Publication, Farmington Hills, MI, USA, 2018.
- [31] G. Campione and F. Cannella, “Engineering failure analysis of corroded R.C. beams in flexure and shear,” *Engineering Failure Analysis*, vol. 86, pp. 100–114, 2018.
- [32] R. A. Hawileh, W. Nawaz, J. A. Abdalla, and E. I. Saqan, “Effect of flexural CFRP sheets on shear resistance of reinforced concrete beams,” *Composite Structures*, vol. 122, pp. 468–476, 2015.
- [33] H. S. S. A. El-Mal, A. S. Sherbini, and H. E. M. Sallam, “Structural behavior of RC beams containing a pre-diagonal tension crack,” *Latin American Journal of Solids and Structures*, vol. 15, no. 7, p. e82, 2018.
- [34] J. S. Jung, B. Y. Lee, and K. S. Lee, “Experimental study on the structural performance degradation of corrosion-damaged reinforced concrete beams,” *Advances in Civil Engineering*, vol. 2019, Article ID 9562574, 14 pages, 2019.
- [35] N. Baša, M. Ulićević, and R. Zejak, “Experimental research of continuous concrete beams with GFRP reinforcement,” *Advances in Civil Engineering*, vol. 2018, Article ID 6532723, 16 pages, 2018.
- [36] GB50010 (2010), *National Standard of the People’s Republic of China. Code for Design of Concrete Structures: GB50010-2010*, China Architecture and Building Press, Beijing, China, 2010, in Chinese.
- [37] J.-Z. Xiao, J.-B. Li, and C. Zhang, “On relationships between the mechanical properties of recycled aggregate concrete: an overview,” *Materials and Structures*, vol. 39, no. 6, pp. 655–664, 2006.
- [38] ACI (American Concrete Institute), *ACI318-08: Building Code Requirements for Structural Concrete and Commentary*, ACI, Farmington Hills, MI, USA, 2008.
- [39] W. Y. Lu, I. J. Lin, S. J. Hwang, and Y. H. Lin, “Shear strength of high-strength concrete dapped-end beams,” *Journal of the Chinese Institute Of Engineers*, vol. 26, no. 5, pp. 671–680, 2003.
- [40] I.-J. Lin, S.-J. Hwang, W.-Y. Lu, and J.-T. Tsai, “Shear strength of reinforced concrete dapped-end beams,” *Structural Engineering and Mechanics*, vol. 16, no. 3, pp. 275–294, 2003.
- [41] K.-H. Yang, H.-S. Chung, E.-T. Lee, and H.-C. Eun, “Shear characteristics of high-strength concrete deep beams without shear reinforcements,” *Engineering Structures*, vol. 25, no. 10, pp. 1343–1352, 2003.
- [42] A. Cladera and A. R. Mari, “Experimental study on high-strength concrete beams failing in shear,” *Engineering Structures*, vol. 27, no. 10, pp. 1519–1527, 2005.
- [43] J. Zhao, J. Liang, L. Chu, and F. Shen, “Experimental study on shear behavior of steel fiber reinforced concrete beams with high-strength reinforcement,” *Materials*, vol. 11, no. 9, p. 1682, 2018.



Hindawi

Submit your manuscripts at  
[www.hindawi.com](http://www.hindawi.com)

